Infrared Physics & Technology 55 (2012) 263–269

Contents lists available at SciVerse ScienceDirect

Infrared Physics & Technology

journal homepage: www.elsevier.com/locate/infrared

Improved interframe registration based nonuniformity correction for focal plane arrays

Chao Zuo *, Qian Chen, Guohua Gu, Xiubao Sui, Jianle Ren

Jiangsu Key Laboratory of Spectral & Intelligence Sense, Nanjing University of Science and Technology, Nanjing, Jiangsu Province 210094, China

ARTICLE INFO

Article history:
Received 18 January 2012
Available online 22 April 2012

Keywords:
Nonuniformity correction
Focal plane arrays
Interframe registration
Fixed pattern noise

ABSTRACT

In this paper, an improved interframe registration based nonuniformity correction algorithm for focal plane arrays is proposed. The method simultaneously estimates detector parameters and carries out the nonuniformity correction by minimizing the mean square error between the two properly registered image frames. A new masked phase correlation algorithm is introduced to obtain reliable shift estimates in the presence of fixed pattern noise. The use of an outliers exclusion scheme, together with a variable step size strategy, could not only promote the correction precision considerably, but also eliminate ghosting artifacts effectively. The performance of the proposed algorithm is evaluated with clean infrared image sequences with simulated nonuniformity and real pattern noise. We also apply the method to a real-time imaging system to show how effective it is in reducing noise and the ghosting artifacts.

1. Introduction

Focal plane array (FPA) sensors, especially infrared FPA (IRFPA) sensors, are widely used in military applications, environmental monitoring, scientific instrumentation, and medical imaging applications [1]. The performance of FPA is known, however, to be strongly affected by fixed pattern noise (FPN), which results from the fact that the responses of different detectors of the array are not identical [1,2]. This noise, which is also referred to as nonuniformity, is especially problematic in IRFPA systems. The overall effect of nonuniformity is that the image is observed as if one is looking through a dirty window. Furthermore, this problem cannot be solved by a one-time factory calibration since the nonuniformity often drifts in time. This slow temporal drift in the pixel response is generally attributed to factors such as variation in the surrounding temperature, changes in the scene, and variation in the transistor bias voltages [2,3]. Reference-based nonuniformity correction (NUC) using uniform blackbody irradiance sources on startup cannot solve the drift in the parameters of the detectors over time. As a result, scene-based nonuniformity correction (SBNUC) methods have been studied to continuously correct IR nonuniformity without interrupting the scene acquisition.

Scene-based algorithms are generally identified by two main approaches: namely, statistical methods [2–7] and registration based methods [8–11]. Statistical techniques typically exploit some spaciotemporal assumptions on the irradiance observed by each detector. One common statistical assumption is constant statistics [4], which states that the statistics of the observed scene become constant over time. So the statistical approaches usually require a significant number of image frames and the camera needs to move in such a way as to satisfy the statistical assumptions [5]. Registration based methods do not use or require any statistical assumptions about the scene and could estimate the nonuniformity in a much smaller number of image frames. These methods consider that each detector should have identical response when observing the same scene point [8–11]. Therefore, registration-based methods require accurate estimation of the motion between frames. Due to its relevance to this paper, we now focus on a registration based algorithm so-called interframe registration based least-mean-square-error algorithm (IRLMS) that was recently developed by Zuo et al. [11]. This technique minimizes the mean square error between two properly registered image frames to make any two detectors with the same scene produce the same output value. It has been reported to be superior to the existing methods and can achieve excellent NUC results with small computational load and memory requirement.

Nevertheless, this technique is not trouble-free and the following issues that are often encountered in practical applications: (1) reliable registration between frames in the presence of FPN; (2) local motion; (3) complex motion fields between consecutive frames. In the IRLMS method, registration is performed by measuring the relative motion between frames via traditional phase correlation methods. But a significant level of FPN makes it difficult to reliably compute the motion between frames. The reason is that dominant components used for motion estimation are mainly from FPN rather than features of real scene motion. Besides, since IRLMS is based on the translation-only registration, its correction accuracy

* Corresponding author.
E-mail address: surpasszuo@163.com (C. Zuo).

1350-4495/$ - see front matter
http://dx.doi.org/10.1016/j.infrared.2012.04.002

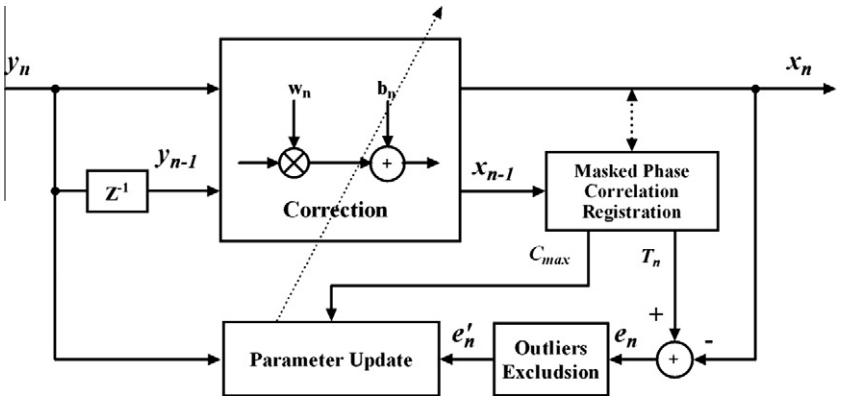

Fig. 1. Block scheme of the proposed NUC method. y_n is the current observed frame and y_{n-1} is the previous observed frame. w_n and g_n are the NUC parameters. x_{n-1} and x_n is the corrected versions of y_n and y_{n-1}, which are properly registered using masked phase correlation method. The error signal e_n is their corresponding difference. The outliers in the error signal e_n are excluded for reliably updating the FPN correction parameters and the phase correlation peak value $c_{\max}$ determines the step size of the current frame.

may be affected by errors resulting from inaccuracy of registration, local motion, scene warping and rotation, etc.

The goal of this paper is to present a novel SBNUC algorithm that provides the key advantages of fast convergence and minor residual error by improving the IRLMS method. Since the performance of registration based algorithms depends heavily on the accuracy of the registration estimates, the very first thing we should do is to improve the accuracy of registration under conditions of nonuniformity noise. Secondly, the IRLMS method is based on the assumption that the radiation emanating from the scene does not change during the time between image frames, which is of course not true when some of the objects in the scene are not motionless. These outlier values caused by local motion should be excluded to prevent a large degree of influence on NUC parameters. Finally, since only translational motion between two image frames is taken into consideration, the estimation errors may result from scene rotation, warping, etc. These errors can be reduced by attenuating these frames' contribution to the updating process.

The remainder of this paper is organized as follows. In Section 2 the proposed scene-based algorithm is presented. In particular, we describe the details of our improvements concerning three aspects on the IRLMS method. After presenting experimental results on synthetic and real data in Section 3, we conclude our paper in Section 4.

2. Proposed method

The NUC algorithm proposed here bases on the same framework as the IRLMS method but has the following improvements: first, we develop a masked phase correlation algorithm for robust motion estimation in the presence of FPN; second, a new decision rule based on the spatial statistics of the calculated error images is designed to exclude the abnormal data which may results from local motion or registration error; finally, a variable step size strategy is employed in the recursive parameter update process to permit a better and more stable estimation for NUC parameters. The intact principle scheme of the proposed algorithm is clearly illustrated in Fig. 1.

Generally, the relationship between the signal response and the incident infrared photon flux is nonlinear, especially when the FPA operates on a wide dynamic incident flux range [12]. For SBNUC, to simplify the problem formulation, the photo-response of the individual detectors in a FPA is commonly approximated to a linear irradiance-voltage model [13] and their output is given by

$$y_n(i,j) = g_n(i,j)\cdot x_n(i,j) + o_n(i,j). \tag{1}$$

Here, subscript n is frame index. $g_n(i,j)$ and $o_n(i,j)$ are respectively the real gain and offset of the (i,j)th detector. $x_n(i,j)$ stands for real incident infrared photon flux collected by the respective detector. This model is reasonable especially for some SBNUC methods with a fast convergence rate, because during a short period of time, the objects temperature could be ensured in a small range so as to satisfy the linear response model. We apply a linear mapping to the observed pixel value to provide an estimate of the true scene value so that the detectors appear to be performing uniformly.

$$x_n(i,j) = w_n(i,j)\cdot y_n(i,j) + b_n(i,j), \tag{2}$$

where $w_n(i,j)$ and $b_n(i,j)$ are respectively the NUC gain and offset of the linear correction model of the (i,j)th detector. Their relations with the real gain and offset can be represented by:

$$w_n(i,j) = \frac{1}{g_n(i,j)}, \tag{3}$$

$$b_n(i,j) = -\frac{o_n(i,j)}{g_n(i,j)}. \tag{4}$$

However, for SBNUC, obtaining the NUC gain and offset is blind estimation because the real gain and offset are known. In IRLMS, the estimation of NUC parameters is achieved by minimizing the mean square error between the two properly registered image frames using the steepest descent method [11]. The needed error image e_n can be formulated as

$$e_n(i,j) = \hat{x}_n(i,j) - T_n(i,j), \tag{5}$$

where $\hat{x}_n(i,j)$ is the nth estimated true image and can be calculated by

$$\hat{x}_n(i,j) = \hat{w}_n(i,j)\cdot y_n(i,j) + \hat{b}_n(i,j), \tag{6}$$

where $w_n(i,j)$ and $b_n(i,j)$ are respectively the estimated gain and offset of the linear correction model of the (i,j)th detector at nth frame. The desired target value $T_n(i,j)$ in Eq. (5) is only a properly shifted version of last frame corrected using estimated parameters:

$$T_n(i,j) = |\Im^{-1}[\Im(\hat{x}_{n-1})e^{-2\pi j(u\delta_x + v\delta_y)}]|, \tag{7}$$

where

$$\hat{x}_{n-1}(i,j) = \hat{w}_n(i,j)\cdot y_{n-1}(i,j) + \hat{b}_n(i,j). \tag{8}$$

The $\Im$ sign indicates the discrete Fourier transform (DFT) and $\Im^{-1}$ represents the inverse DFT operation. (u, v) are the Fourier domain coordinates. The DFT and its inverse can be computed efficiently using fast Fourier transform. The (δ_x, δ_y) represents the translation

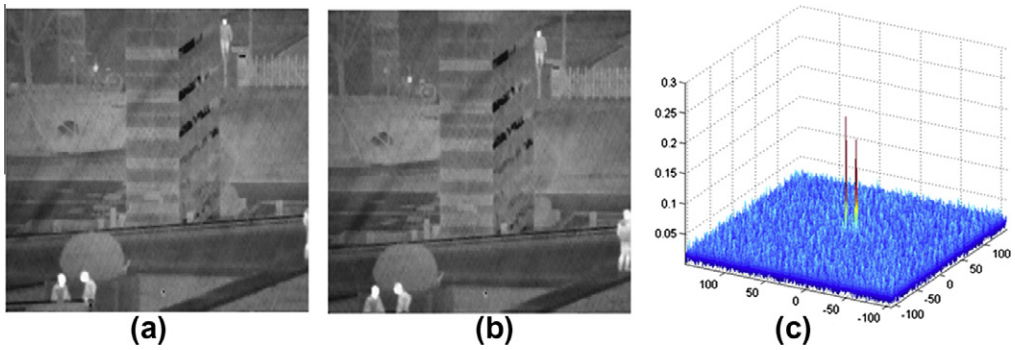

Fig. 2. Two noisy infrared images with some shifts (shown in (a) and (b)) and their phase correlation matrix (shown in (c)). Two distinctive peaks correspond to the FPN and the real scene motion, respectively.

(in pixels) between the two adjacent frames (frame n and frame $n-1$), which can be obtained using masked phase correlation registration algorithm. Some details about this algorithm will be given in Section 2.1. After we get the error image e_n, a post-processing procedure is needed to exclude some outliers. This part will be discussed at length in Section 2.2. The modified error image is denoted as e'_n. The parameter update process is finally described as follows:

$$\begin{cases} \hat{w}_{n+1}(i,j) = \hat{w}_n(i,j) + \alpha_n \cdot e'_n(i,j) \cdot y_n(i,j) \\ \hat{b}_{n+1}(i,j) = \hat{b}_n(i,j) + \alpha_n \cdot e'_n(i,j) \end{cases} \tag{9}$$

Note that the NUC parameters are only updated in the overlapped part between frame $n-1$ and frame n. In our method, the step size α_n is adapted to the scene content and depended on the value of phase correlation peak. This step will be discussed in Section 2.3.

Finally, it should also be mentioned that for some high-frame-rate infrared cameras, almost no translation between two frames can be detected in most cases. If we still use two adjacent frames to register, the NUC performance will obviously degenerate. So in this paper, the above update process is performed only if a sufficient displacement (2 pixels used in [11]) is measured between the current frame (frame n) and a reference frame (frame $n-k, k = 1, 2, 3, \ldots$). And the reference frame is only refreshed when the correction coefficients are updated.

2.1. Masked phase correlation registration

The phase correlation registration enables to estimate the displacement between images with subpixel accuracy from the location of the phase correlation peak [14]. The peak is a Dirac delta function in continuous case. While in the discrete case, it is a Dirichlet kernel [15]. Subpixel Registration can be effectively achieved by the upsampled correlation peak using matrix-multiply DFT [16]. However, as mentioned earlier, conventional registration techniques are difficult to obtain reliable estimates of motion between frames under significant FPN.

Considering the case where the offset FPN is the dominate noise in the captured images and the changes in dynamic range of incident infrared flux are rather small during the interframe time, in the registration procedure, we simplify the detector response model, assuming that the influence of the gain nonuniformity can be neglected. This simplification is crucial because if the gain component is involved, the FPN will become signal dependent, making our registration problem to be a very hard nut to crack. We found that this simplification is reasonable and its validity was verified via several experiments. Using this offset-only model, the two consecutive image frames f_1 and f_2 can be represented as follows:

$$f_1(i,j) = x(i,j) + o(i,j), \tag{10}$$

and

$$f_2(i,j) = x(i+\delta_x, j+\delta_y) + o(i,j). \tag{11}$$

The FPN $o(i,j)$ is assumed to be fixed between two observed images and signal independent. (δ_x, δ_y) is the scene relative translation (in pixels) between the two images. Then the normalized (whiten) cross-power spectrum can be expressed as:

$$\begin{aligned} C(u,v) &= \frac{\Im(f_1)\Im^*(f_2)}{|\Im(f_1)\Im^*(f_1)|} \\ &= \frac{|\Im(s)|^2}{|\Im(s)|^2 + |\Im(o)|^2} e^{-j(u\delta_x + v\delta_y)} + \frac{|\Im(o)|^2}{|\Im(s)|^2 + |\Im(o)|^2}, \end{aligned} \tag{12}$$

where the asterisk stands for the complex conjugate. In such circumstances, the phase correlation matrix $c(x,y) = |\Im^{-1}[C(u,v)]|$ is no longer a Dirac delta function but two peaks with magnitudes related to the corresponding frequency content (see Fig. 2). According to the convolution theorem and the properties of Fourier transform, we know that the two peaks must be highly spatial limited and with narrow support. Since the FPN is motionless, one of the intensity peaks in the image $c(x,y)$ is always located at the origin (0, 0), while the coordinate of the other peak corresponds directly to the translation vector (δ_x, δ_y). This makes it easier to identify the true scene motion. However, when the displacement is too small, two peaks may be too close to be resolved. Fortunately, the nonuniformity coefficients are only updated if sufficient displacement (2 pixels) is measured. So we can first mask the origin and its four nearest neighbor pixels in $c(x,y)$ with zeros, and then search for the second peak. If the amplitude of second peak $c_{\max}$ is too small (<0.05), which means the relative displacement is insufficient, no update is preformed for this frame. Otherwise, we upsample the second correlation peak using matrix-multiply DFT [16] to get an estimate of the real scene displacement with subpixel accuracy. In this paper, the upsampling factor is chosen as 10, which means the registration accuracy can reach 0.01 pixel, theoretically. The flowchart of the proposed masked phase correlation registration method is illustrated in Fig. 3.

2.2. Exclude the abnormal data

The IRLMS method assumes that the temperature field of the observed scene does not change during the interframe time interval. However, if the objects in the scene are not motionless, this assumption cannot be met well so that real scene information may leak into the error signal. Hence the error signal is unreliable in the local motion region and the correction coefficients would be wrongly updated. In addition, the registration errors may make this matter even worse, severely affecting the NUC precision.

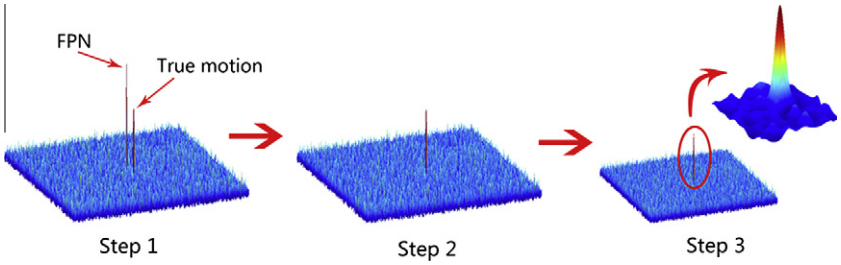

Fig. 3. Flowchart of the masked phase correlation registration algorithm: Step 1: Calculate the phase correlation matrix; Step 2: Mask the origin region; Step 3: Identify the true peak and upsample it using matrix-multiply DFT to obtain its coordinate with subpixel accuracy.

Statistically, the nonuniformity in the gains and offsets of individual detectors due to temporal drift are often modeled as independent and identically distributed Gaussian random process [8,17]. Although this model is not so accurate because the FPN is usually perceived as a grid-like pattern or as a striping pattern laid on top of the true scene [18], when the gain/offset parameters are histogramed, their value distribution will be approximately Gaussian. Using this regulation, the error image can also be assumed to obey a Gaussian distribution with mean μ_n and standard deviation σ_n, where the μ_n and σ_n are the spatial mean and standard deviation of the error image, respectively. However, the error caused by local motion is obviously deviated from the Gaussian distribution. For global registration error, the situation is more complicated. Due to the spatial correlation of the observed scene, most pixels' values are rather similar with those of their neighborhoods. In these homogeneous regions of the scene, the effect of registration error is slight. While in the strong edges objects in the scene, the influence of registration error is vital. The Gaussian distribution prior is also very useful to identify those "dangerous pixels" around scene edges. So we can exclude the abnormal data based on the following rules:

$$e'_n(i,j) = \begin{cases} 0 & \text{when} |e_n(i,j) - \mu_n| \geqslant 3\sigma_n \\ e_n(i,j) & \text{when} |e_n(i,j) - \mu_n| < 3\sigma_n \end{cases} \tag{13}$$

It can be seen when the value of the error image has a greater difference from the expectation, it will be set to zero and no updating will be done. This mechanism prevents biased estimates from improper updating caused by the outliers and helps to sample data better. Fig. 4 gives an example to demonstrate the effect of the proposed scheme. Fig. 4a and b are two consecutive frames taken from a noisy infrared sequence. Note that the FPN is superimposed on the scene. There are also a number of bad pixels. The two people in the camera view were on a walk during the shoot, so their contours are clearly outlined in the error image shown in Fig. 4d. We hope that the error image contains only nonuniformity, and the scene information can be erased as much as possible. The bad pixel should also be excluded to produce an unbiased error image. From Fig. 4c, it can be seen that the values of error image can be approximately regarded as a Gaussian distribution. Using the "$3\sigma_n$ principle", we detect these abnormal data and bad pixels, successfully (Fig. 4e). The final modified error image is shown in Fig. 4f. It can be seen that the pixel values in error regions are set to null, thus no parameter updating would be performed in these regions. The

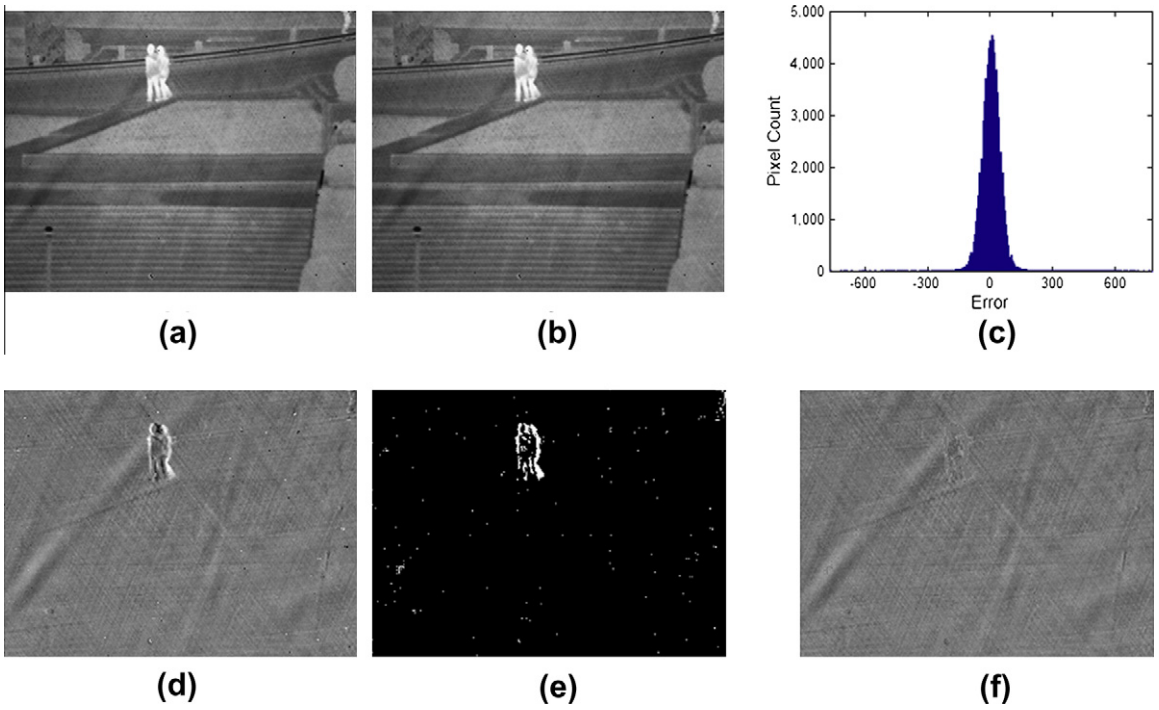

Fig. 4. Exclude the outliers from the error image. (a) and (b) Are two adjacent frames taken from a sequence of IR data. (c) Is the interframe error distribution and (d) is the error image (overlapped region only). The detected the abnormal data (shown in white) and the modified error image are shown in (e) and (f), respectively.

modified error image shows very little scene information so that no significantly wrong updating would happen, preventing perceivable ghosting emerging.

2.3. Variable step size

The parameter α in the IRLMS represents the step size of the algorithm and governs the convergence speed. Normally, larger values for α can provide a faster convergence speed, but smaller values can assure better stability instead. The adaptive step size strategies are widely adopted to improve the performance of the Scribner's method [17,19,20]. The main idea behind these strategies is to adjust the step size based on local spatial variance of the observed image. If a given piece of the input image (a pixel and its neighbors) is smooth enough, then the desired averaged target value at the output is more confident, and the step size assumes larger values. On the other hand, if the local input standard deviation in the surroundings of a certain pixel is too high, like in an object border, the correspondent step size assumes smaller values.

Inspired by these strategies, we also employed the variable step size rule to increase the efficiency of the parameter updating process of IRLMS. Specifically in the IRLMS, the error confidence is directly dependent on how well the two adjacent frames are matched. Under ideal circumstances, i.e. there is a one-to-one mapping of pixels map between two images; the height of a phase-correlation peak is unity. Because of the FPN, usually there are two peaks in the phase-correlation function in our condition; the sums of the two peaks should be unity ideally. However, some factors such as local motion, scene rotation, warping, and other perturbations may diminish the value of the phase-correlation peak at the correct displacement position [14]. These factors also cause estimation errors in the updating process. Obviously, the error signal measure is more reliable when the objects in the scene are stationary and the motion between current image and the reference image is pure translation. In this case, large values of α should be used. On the other hand, when there is rotation or warping between two consecutive frames or the scene is very busy, the error image may contain more scene information and there will be more chances to deviate the parameters estimation. In such situations, α should assume smaller values. Considering the amplitude of the coherent peak $c_{\max}$ at the true shift position in the phase correlation matrix is a direct measure of the degree of congruence between the two images, α_n can be adaptively controlled as follows:

$$\alpha_n = a_{\max} \times c_{\max}, \tag{14}$$

where $a_{\max}$ denotes the maximal iterative step size which range from 0 to 1 (we use 0.05 as recommended in [11]) and $c_{\max}$ is the value of the coherent peak corresponding to the true shift in the phase correlation matrix. Besides, the initial convergence should not be affected by the noisy phase correlation matrix, so we use $\alpha_n = a_{\max}$ for the first 50 times updates. When the FPN is largely removed, the convergence is controlled by the value of the phase correlation peak.

3. Results

To validate the effectiveness of the proposed method, we first compared it with IRLMS by using a 500-frame IR video sequence I with simulated nonuniformity. The test sequence I was collected by using a properly calibrated 320 × 256 HgCdTe IRFPA camera operating in the 8–14 μm range and working at 25 frames per second (FPS), corrupted with a synthetic gain with a unit-mean Gaussian distribution with standard deviation of 0.1, and a synthetic

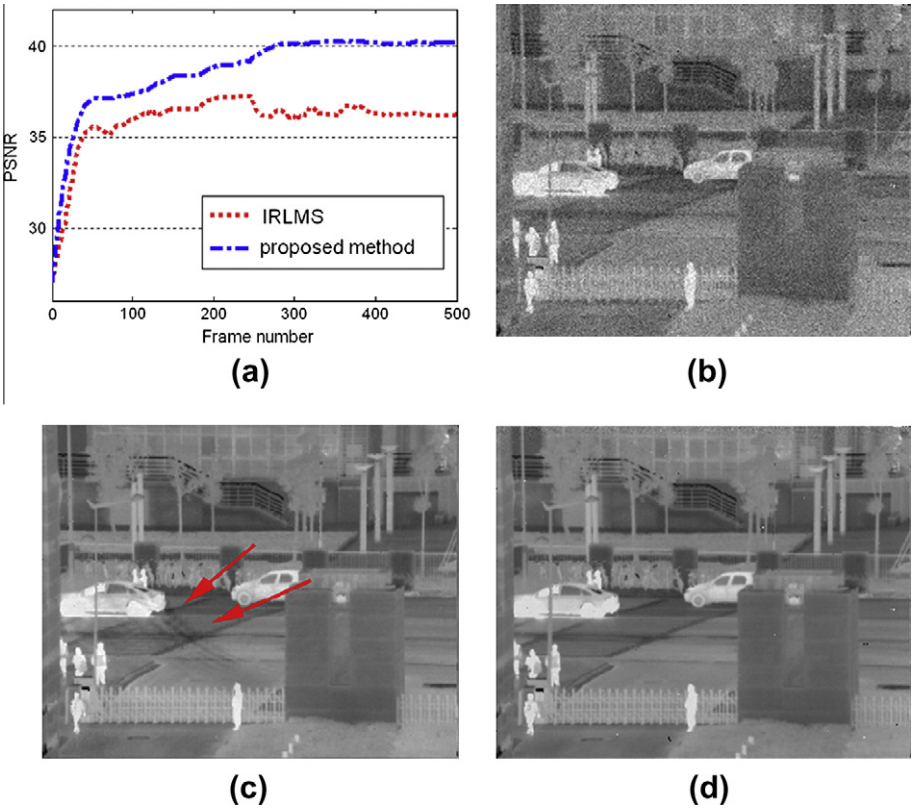

Fig. 5. PSNR results of the synthetic noisy test sequence I (a). (b) Is the raw 400th frame in the test sequence and (c) and (d) are the correction results of the IRLMS and the proposed method.

offset with a zero-mean Gaussian distribution with standard deviation of 50. The metric used to measure the NUC performance is given by the peak signal-to-noise ratio (PSNR), which is widely used to quantify the differences between two images, and it is defined as

$$\mathrm{PSNR} = 20\log_{10}\left(\frac{2^b - 1}{\mathrm{RMSE}}\right), \tag{15}$$

where b represents the number of bits per pixel in the image, which in this case is equal to 14. RMSE is the root mean square error of the difference between two images, which is defined as

$$\mathrm{RMSE} = \sqrt{\frac{1}{M \cdot N}\sum_{i,j}[x(i,j) - \hat{x}(i,j)]^2}, \tag{16}$$

where $x(i,j)$ is the (i,j)th pixel's value of the true frame while $\hat{x}(i,j)$ is the pixel's value of the corrected frame. M and N are the image dimensions. The PSNR is finally given in decibel units (dB), and it measures the overall difference between a clean reference image against its nonuniformity corrected version. Larger values for the PSNR indicate better NUC performances.

The PSNR evolution of the two tested algorithms is displayed in Fig. 5a. It can be seen clearly that the proposed method achieves faster convergence and minor residual error compared with the IRLMS method. For the first 50 frames, the curve of the proposed method rose faster, because sometimes the IRLMS failed to detect the real translation between two dirty images, wrongly considering the motion was insufficient, which slowed its parameter updating process. For the rest of the sequence, the PSNR of the proposed method kept at a high level, especially for the last 300 frame, it is about 4 dB greater than that of the IRLMS.

To better explain the gap in PSNR, the resulting video sequence I (Video 1) and one sample frame was presented. In Fig. 5b–d, an example of the corrupted, and the corrected IR images obtained with two methods tested can be observed. It can be noted that, to the naked eye, the proposed produces a better NUC result than the IRLMS method. Again, a visual inspection of Video 1 shows that the image corrected with our algorithm is much less affected by the ghosting caused by the objects with local motion than the one corrected with the IRLMS method, which explains in part the higher performance rates achieved.

In the above simulation, the nonuniformity was assumed to be spatially unstructured random variables and the camera was panned horizontally/vertically. In the second simulation, we focus on the conditions that the nonuniformity is structured pattern and the motion is more complex. The noise pattern shown in Fig. 6a is the FPN acquired from a real 320 × 256 uncooled IRFPA camera. Another 300-frame clean IR video sequence was captured and we vary the amounts of the added FPN to produce the test sequence II with a PSNR around 27. One sample corrupted image is shown in Fig. 6b. Since only offset nonuniformity is considered in this simulation, we applied an offset-only version of our NUC method to this corrupted sequence. To show how the variable step size strategy can help prevent abnormal updating in NUC parameters, we illustrate the evolution of step-size α_n in Fig. 6c. The PSNR evolution is shown in Fig. 6d and the resulting video sequence (Video 2) was presented as well. At first 100 frames, the camera moved horizontally/vertically. From frame 100–270, we turned the camera upside down several times to create complex motions. From Fig. 6c, it can be seen that the step-size value kept at a low-level (generally < 0.01) during frame 100–270, preventing NUC parameter wrongly update. Meanwhile, although the PSNR fluctuated during these frames, it still kept above 37.5 dB. After that stage, the value of PSNR continued to rise, reaching 39.7 dB at the last frame. The correction video and PSNR result shows that the proposed method can tackle complex motion and structured nonuniformity without affecting the NUC precision.

To demonstrate the performance of the proposed NUC method in a practical imaging system, a real-time correction video (Video 3) is also captured by using a 320 × 240 VOx uncooled microbolometer. Our method has been fully implemented on a Texas Instruments DM642 digital signal processor, working at 25 FPS (25 Hz PAL). Two photos of the camera core with the hardware are shown in Fig. 7.

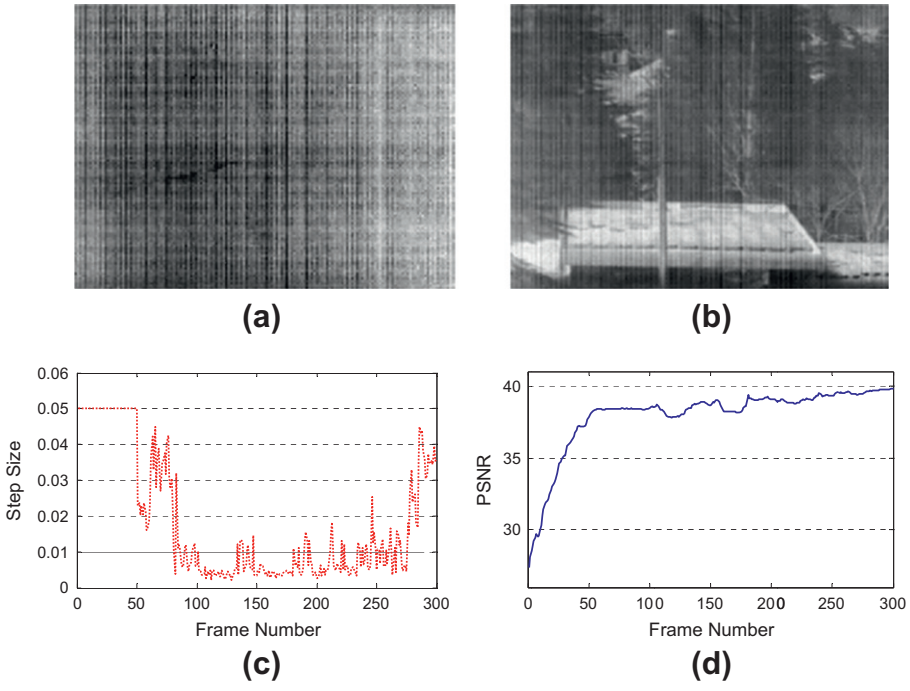

Fig. 6. A real nonuniformity pattern (a) and a sample frame of simulated corrupted sequence (b). (c) Is the evolution curve of the step size. (d) Is the PSNR results of test sequence II.

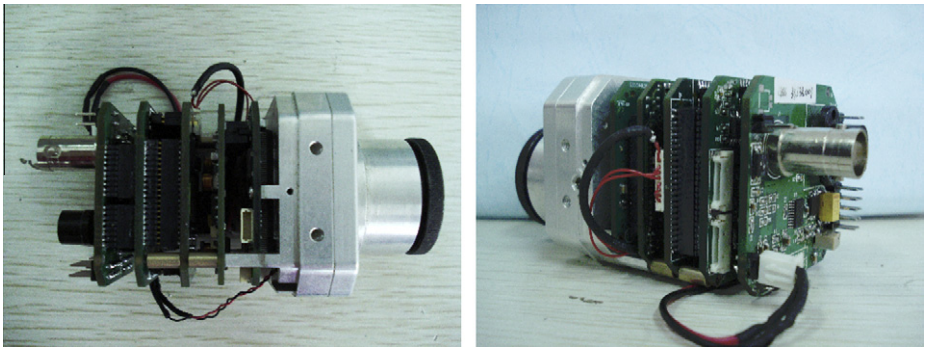

Fig. 7. The 320 × 240 VOx uncooled camera core with the hardware.

The correction video has been acquired inside a laboratory. During the capture, the camera is held by hand. The 14 s sequence does not present a sufficient global motion. Moreover, the human in the field of view was in continual motion. Despite this challenging situation, our algorithm only required about one second to exhibit an excellent reduction of FPN. The subsequent corrected images showed a clear scene, and the residual nonuniformity was scarcely perceptible. Besides, almost no ghosting artifact could be detected through the whole sequence.

4. Conclusion

We have presented a novel scene-adaptive NUC algorithm based on interframe registration. Such an algorithm employs masked phase correlation method to calculate the motion between two consecutive frames, which results in more reliable and robust translation estimates than traditional registration methods under conditions of FPN. In addition, a decision rule is introduced to exclude the abnormal data in the error image, which promotes the correction precision considerably. Finally, the parameters updating process is well controlled by adjusting the step size coefficient according to the amplitude of the phase correlation peak. Those improvements contribute to the performance and robustness promotion of our algorithm. The quantitative error analysis showed that the improved method had faster convergence rate than the IRLMS methods, as well as higher overall PSNR. Moreover, the high-quality correction abilities of the presented method were demonstrated through simulations and application to real uncooled IRFPA sensors.

Acknowledgments

The authors would like to thank Shijie Feng and Fangxiaoyu Feng for proofreading this paper. This work was supported by the Research and Innovation Plan for Graduate Students of Jiangsu Higher Education Institutions, China (Grant No. CXZZ11_0237) and National Natural Science Foundation of China (Grant No. 61101119).

Appendix A. Supplementary material

Supplementary data associated with this article can be found, in the online version, at http://dx.doi.org/10.1016/j.infrared.2012.04.002.

References

[1] D.A. Scribner, M.R. Kruer, J.M. Killiany, Infrared focal plane array technology, Proc. IEEE 79 (1991) 66–85.
[2] D.A. Scribner, K.A. Sarkady, M.R. Kruer, J.T. Caulfield, J.D. Hunt, M. Colbert, M. Descour, Adaptive retina-like preprocessing for imaging detector arrays, in: Neural Networks, 1993, IEEE International Conference, vol. 1953, 1993, pp. 1955–1960.
[3] C. Zuo, Q.A. Chen, G.H. Gu, W.X. Qian, New temporal high-pass filter nonuniformity correction based on bilateral filter, Opt. Rev. 18 (2011) 197–202.
[4] J.G. Harris, C. Yu-Ming, Nonuniformity correction of infrared image sequences using the constant-statistics constraint, Image Process. IEEE Trans. 8 (1999) 1148–1151.
[5] C. Zuo, Q. Chen, G.H. Gu, X.B. Sui, W.X. Qian, Scene-based nonuniformity correction method using multiscale constant statistics, Opt. Eng. 50 (2011).
[6] A. Rossi, M. Diani, G. Corsini, Temporal statistics de-ghosting for adaptive nonuniformity correction in infrared focal plane arrays, Electron. Lett. 46 (2010) 348–U4869.
[7] D.A. Scribner, K.A. Sarkady, M.R. Kruer, J.T. Caulfield, J.D. Hunt, C. Herman, Adaptive nonuniformity correction for IR focal-plane arrays using neural networks, in: T.S.J. Jayadev (Ed.), SPIE, 1991, pp. 100–109.
[8] R.C. Hardie, M.M. Hayat, E. Armstrong, B. Yasuda, Scene-based nonuniformity correction with video sequences and registration, Appl. Opt. 39 (2000) 1241–1250.
[9] B.M. Ratliff, M.M. Hayat, R.C. Hardie, An algebraic algorithm for nonuniformity correction in focal-plane arrays, J. Opt. Soc. Am. A 19 (2002) 1737–1747.
[10] B.M. Ratliff, M.M. Hayat, J.S. Tyo, Generalized algebraic scene-based nonuniformity correction algorithm, J. Opt. Soc. Am. A 22 (2005) 239–249.
[11] C. Zuo, Q. Chen, G.H. Gu, X.B. Sui, Scene-based nonuniformity correction algorithm based on interframe registration, J. Opt. Soc. Am. A 28 (2011) 1164–1176.
[12] L. Biberman, (Ed.), Electro-Optical Imaging: System Performance and Modeling, SPIE and ONTAR Corp, 2000.
[13] D.L. Perry, E.L. Dereniak, Linear theory of nonuniformity correction in infrared staring sensors, Opt. Eng. 32 (1993) 1854–1859.
[14] C.D. Kuglin, D.C. Hines, The Phase Correlation Image Alignment Method, in: IEEE International Conference on Cybernetics and Society, 1975, pp. 163–165.
[15] H. Foroosh, J.B. Zerubia, M. Berthod, Extension of phase correlation to subpixel registration, IEEE Trans. Image Process. 11 (2002) 188–200.
[16] M. Guizar-Sicairos, S.T. Thurman, J.R. Fienup, Efficient subpixel image registration algorithms, Opt. Lett. 33 (2008) 156–158.
[17] R.C. Hardie, F. Baxley, B. Brys, P. Hytla, Scene-based nonuniformity correction with reduced ghosting using a gated LMS algorithm, Opt. Express 17 (2009) 14918–14933.
[18] O.J. Medina, J.E. Pezoa, S.N. Torres, A frequency domain model for the spatial fixed-pattern noise in infrared focal plane arrays, in: P.D. LeVan, A.K. Sood, P.S. Wijewarnasuriya, M. Razeghi, J.L.P. Vizcaino, R. Sudharsanan, M.P. Ulmer, T. Manzur (Eds.), SPIE, San Diego, California, USA, 2011, pp. 81550H–81559.
[19] S.N. Torres, E.M. Vera, R.A. Reeves, S.K. Sobarzo, Adaptive scene-based nonuniformity correction method for infrared-focal plane arrays, Infrared Imaging Syst.: Des. Anal. Model. Test. Xiv 5076 (2003) 130–139.
[20] E. Vera, S. Torres, Fast adaptive nonuniformity correction for infrared focal-plane array detectors, Eurasip. J. Appl. Sig. P 2005 (2005) 1994–2004.